Pergamon

Int. J. Heat Mass Transfer. Vol. 37, No. 13, pp. 1829–1837, 1994

0017–9310/94 $7.00+0.00

0017–9310(94)E0028–S

Effect of humid air flow rate on the filmwise condensation inside a vertical cooled pipe: numerical and experimental study

C. PELE,† B. BAUDOIN‡ and J. P. BARRAND§

†Ingénieur Cetiat, 27–29 bd du 11 novembre 1918, BP 6068, 69604 Villeurbanne cedex, France;
‡Département Energétique, Ecole des Mines de Douai, 941 rue Charles Bourseul, 59500 Douai, France;
§Laboratoire de Mécanique de Lille, URA CNRS 1330, ENSAM, 8 Boulevard Louis XIV, 59046 Lille cedex, France

(*Received for publication* 8 February 1994)

Abstract—This study consists of evaluating the effect of the saturated humid air flow rate on the heat and mass transfer in a vertical exchanger. One of the affected parameters is the shear stress along the liquid vapor interface. The second studied point is the effect of flow rate on the diffusion of the vapor in the mixture. A simple mathematical model is built from one-dimensional equations for the mass conservation, enthalpy and momentum. In order to validate the model, an experimental apparatus allows to have access to the local heat transfer passing through the wall. The experimental results are in good agreement with the theoretical predictions. They show that the cocurrent gas/liquid flow allows a better recovery of energy.

1. INTRODUCTION

NON-CONDENSING gases are frequently present in most industrial processes where condensation is taking place. So, the problem consists in recovering the gas vapor, by creating conditions of condensation on the cold walls of the condenser.

This study concern the influence of the wet air flow direction on the heat and mass transfer in a vertical condenser.

Due to the action of the thermal gradient, the water vapor condenses and releases latent capacity in the boundary layer. This phase change gives rise to an important heat flux and so increases the heat transfer obtained by forced convection. Nevertheless, the accumulation of non-condensing gas controlled by the diffusion introduces an additional thermal resistance to those existing near the wall in the liquid.

The liquid is influenced by two forces: its weight and the shear stress at the gas–liquid interface. The direction of the air flow, up or down, slows down or speeds up the condensate flow rate, due to the action of the shear stress at the gas–liquid interface, and therefore influences its thickness and behaviour.

The following assumptions are made in the present study:

- the difference between the wall temperature and the mean temperature of the gaseous phase is small;
- the vapor/non-condensing gas mass ratio is small; and
- natural convection is negligible compared to the forced convection.

Industrial condensers are used in this field.

2. LITERATURE SURVEY

The laminar filmwise condensation on a vertical flat plate has been a subject of study since 1915 with the pioneering works of Nusselt. The original model used by Nusselt is built with a vertical plate in a stagnant vapor. The temperature of the plate is uniform and lower than the temperature of the vapor. A laminar film of condensate falls down along the plate due to the gravity, and the condensation occurs only on this film. Subsequently, many changes of this analysis have appeared, each one improving the restrictive assumptions of the Nusselt analysis [1–5].

Owen and Lee [1] summarized the recent developments on the subject of condensation, mainly concerning the numerical models. They classified the different methods by order of complexity:

- Method of the condensation curve based on the equilibrium of the vapor/gas mixture versus the temperature. This method, using the thermodynamic equilibrium without heat and mass transfer, will be used with a condenser operating at low condensation rates because of the small temperature differences between each phase.
- Method of film condensation where mass, heat and momentum transfers are studied in a non-condensing film near the condensate. This method, described by Colburn and Hougen [2] and Colburn and Drew [3], is often used to calculate the industrial condensers because of its applicability to all geometries.
- Method of boundary layer in which the numerical methods are used to solve the general conservation equations.

NOMENCLATURE

co, ct	cocurrent, counter current
C_τ	skin friction coefficient
Cp	specific heat at constant pressure
D	mass diffusivity coefficient
d_h	hydraulic diameter
g	acceleration of gravity
h	heat transfer coefficient with mass transfer
h_D	mass transfer coefficient
h_0	heat transfer coefficient
M	molar mass
m_v	rate of the vapor mass transfer flux
n	0.124, see equation (10)
Nu	Nusselt number
p	pressure
Pr	Prandtl number
q	mass flow rate
r, R	radius (r: radial distance)
$\boldsymbol{R}$	universal perfect gas constant
Re	Reynolds number
s	area
Sc	Schmidt number
T	temperature
T_e	inlet air temperature
u_z	velocity
u, v	components of the velocity
y, z	coordinates (z: vertical tube axis).

Greek symbols

Δ	boundary layer thickness
δ	thickness of the condensate film
λ	thermal conductivity
Λ	Prandtl mixing length
μ	dynamic viscosity
ν	kinematic viscosity
ρ	density
τ	shear stress
Φ	flux.

Subscripts

C	dynamic
D	diffusion
E	water
e	inlet
g	non-condensing gas
i	interface
l	laminar
m	in the core of the mixture
t	turbulent
v	vapor.

3. THEORETICAL ANALYSIS

3.1. *Balance equations in the gas mixture*

The theoretical model is expressed from the mass, energy and momentum balance equations applied to a control volume between the two cross-sections z and $z+\mathrm{d}z$ (see, for example, Fig. 1), with the assumptions that the gaseous phase flow is turbulent and that the pressure is uniform in each section. In these equations, the upper sign concerns the mixture/condensate cocurrent flow and the lower sign applies to the counter current case:

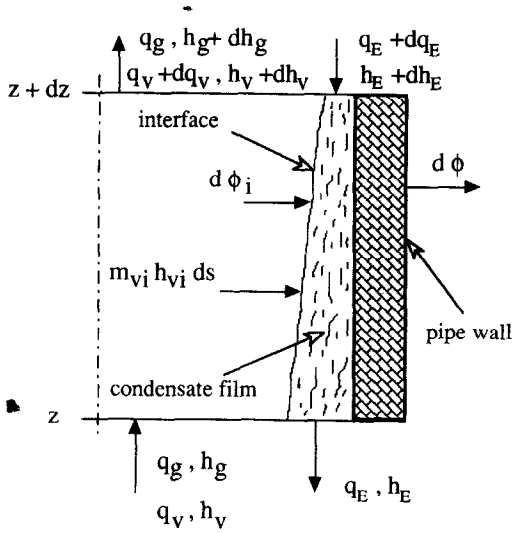

FIG. 1. Control volume and energy balance in the counter current.

mass balance:

$$\mathrm{d}q_v = \pm m_{vi} \quad \mathrm{d}s = \pm \mathrm{d}q_E, \tag{1}$$

energy balance:

$$\mathrm{d}T = \frac{\pm \mathrm{d}\phi_i \pm m_{vi} Cp_v (T_i - T)\,\mathrm{d}s}{q_g Cp_g + q_v Cp_v}, \tag{2}$$

momentum balance:

$$\frac{\mathrm{d}p}{\mathrm{d}z} = \frac{4 U_g m_{vi}}{R_i} \pm 2 \frac{\tau_i}{R_i} - \rho_g g. \tag{3}$$

The last equation shows that the pressure gradient depends on the condensing phase inertial effect, on the shear stress at the interface and on gravity. The coefficient 4 is issued from the derivation of the second order of the mass flow rate and from the simplification of ratio between the interface area and the free flow area.

3.2. *Definition of the local transfer coefficient in the gas mixture*

In the previous balance equations, some unknown parameters must be determined locally in each section. The main unknowns on the heated side are:

- condensation mass flow rate of the vapor per unit wall surface;
- heat flux ϕ_i; and
- shear stress τ_i at the gas–liquid interface.

The determination of these quantities is made with local exchange coefficients. So, the local density of condensated vapor mass flux can be determined by defining a mass transfer coefficient such as:

$$m_{vi} = h_D \frac{pM_v}{RT} \frac{p_{vm} - p_{vi}}{p - p_{vm}}. \quad (4)$$

This definition is similar to the one used by Bird *et al.* [5]. The heat transfer ϕ_i is determined by defining a convection coefficient with mass transfer as:

$$\phi_i = h(T_m - T_i)s. \quad (5)$$

The determination of h is obtained from the Colburn analogy:

$$Nu = 0.023 Pr^{1/3} Re^{4/5}$$

with $\quad Nu = h_0 d_h/\lambda \quad$ and $\quad Re = u(2R_i)/v,$

where h_0 is the heat transfer coefficient without mass transfer, R_i is the radius from the gas–condensate interface to the tube center, and u is the average velocity of the mixture; h and h_0 are related by:

$$h = h_0 \frac{a}{1 - e^{-a}} \quad \text{with} \quad a = \frac{m_{vi} Cp_v}{h_0}.$$

In the condensation of humid air, the mass transfer is low and the heat transfer coefficient may therefore be assimilated to h_0: $h \to h_0$. For the shear stress at the interface, we define a drag coefficient:

$$\tau_i = 0.5 C_\tau \rho_m (u_m - u_i)^2,$$

then, as the liquid velocity at the interface is neglected with respect to the gaseous phase velocity:

$$\tau_i = 0.5 C_\tau \rho_m u_m^2, \quad (6)$$

with

$$C_\tau = 0.079 Re^{-1/4}.$$

We suppose that condensation has no influence on this coefficient.

It is necessary to determine the parameters at the interface. They should be known after the evaluation of the thermal resistances, of the condensate and of the non-condensing gas film. These thermal resistances in series are respectively determined from the Nusselt equation, in which the shear stress is not neglected, and with the modeling of the turbulent diffusion coefficient.

3.3. *Condensate flow*

The velocity profile within the liquid laminar film falling along the tube wall assimilated to a vertical flat plate and taking into account the pressure gradient and the interface shear stress is:

$$u_E(y) = -\frac{1}{\mu_E}\left[\left(g\rho_E - \frac{dP}{dz}\right)\left(\delta - \frac{y}{2}\right)y \pm \tau_i y\right]. \quad (7)$$

From this equation, we can determine the variation of the condensate mass flow rate along z which must be equal to the variation of vapor flow rate, in each section. The thickness of the condensate film is deduced from this relation.

3.4. *Modeling of the diffusivity coefficient*

The diffusivity coefficient is the sum of the molecular and turbulent transport contributions. The molecular or laminar coefficient is linked to the local temperature by the Schirmer formula [7]. In order to calculate and to model the turbulent diffusivity, we use the Prandtl mixing length which assumes a similarity between the turbulent viscosity and the turbulent diffusivity. So we can link by the turbulent Schmidt number:

$$Sc_t = v_t/D_t. \quad (8)$$

The turbulent viscosity is linked to the mean velocity gradient by the following relation:

$$v_t = \Lambda^2 \frac{du_z}{dy}, \quad (9)$$

where Λ is the Prandtl mixing length. For moderate condensation rate, Λ is independant of the mass transfer. Nevertheless, in the viscous sublayer and in the buffer layer, this theory is no more valid so we use the Deissler's equation [6]:

$$v_t = n^2 u_z y [1 - \exp(-n^2 u_z y/v_l)]. \quad (10)$$

This set of equations, (8)–(10), forms the turbulence model used in our calculations.

3.5. *Axial evolution of the boundary layer of diffusivity*

The turbulent flow is uniform, but the condensation begins at the abscissa z_0. It is necessary to take into account the development of the boundary layer of diffusivity along the interface. So we use the film model which assumes that the main part of the heat and mass exchanges are located near the interface. Thus, the mass transfer coefficient is written as $h_D = D_{eff}/\Delta_0$, Δ_0 being the thickness of the diffusion boundary layer when the boundary layers are fully developed. The Reynolds analogy suggests that the ratio between the velocity boundary layer and diffusion boundary layer is equal to the cubic root of the Schmidt number. But if the diffusivity boundary layer develops from the abscissa z_0 the ratio becomes:

$$\left[\frac{\Delta_D(z)}{\Delta_C}\right]^3 = \frac{1}{Sc}\left[1 - \left(\frac{z_0}{z}\right)^{3/4}\right]. \quad (11)$$

The mass transfer coefficient is written:

$$h_D(z) = \frac{h_D}{\left[1 - \left(\frac{z_0}{z}\right)^{3/4}\right]^{1/3}}. \quad (12)$$

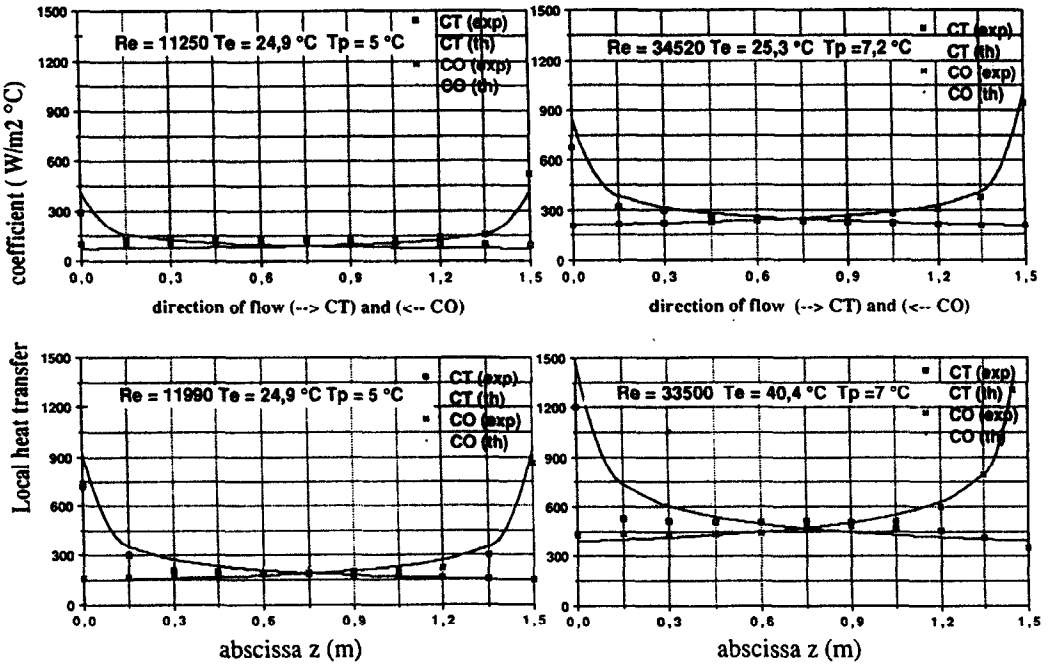

FIG. 2. Comparison of two flow directions.

h_D is the mass transfer coefficient when the diffusivity boundary layer is fully developed.

3.6. *Numerical resolution*

The numerical resolution is made by integrating the balance equations with a fourth-order Runge–Kutta method. The temperature at the interface is determined using the Newton method by imposing the equality between the heat flux of the mixture at the interface and the one going through the wall. The condensate thickness is determined by dichotomy equalizing the variations of the condensate flow rate and the vapor flow rate. The theoretical axial distribution of the local exchange coefficient is shown in Fig. 2. The gas–condensate cocurrent flow increases the heat and mass exchanges. Moreover, the exchanges are influenced by the tube inlet, mainly in the cocurrent mode.

4. EXPERIMENTAL STUDY

4.1. *Measurement of local heat flux in a tubular condenser*

An experimental apparatus was designed in order to study the effect of the gas flow direction. Only the air and water supply was changed to modify the flow direction.

Figure 3 presents the main part of the experimental setup. The air circuit is supplied by a compressor. The air flow is measured after expansion by a flowmeter. This air is saturated in humidity by water paddling. The air temperature is maintained constant during the test. After that, this humid air successively enters in a settling chamber and in the test section. The experimental condenser in "PVC" consists of two coaxial tubes 1.5 m length. The inner diameter is 33.5 mm and the diameters of the annular section are 40 and 120 mm. The length of the settling chamber, with the same diameter as the condenser, is 1.5 m. The "PVC" was made "water absorbent" by a specific treatment (oxidising plasma). Moreover, in order to make it perfectly wettable, before an experiment, the surface is coated with a wet chemical product diluted in water ("coptal"). When the surface is dry, the experiment can be carried out. The condensate is collected in the lower part of the surface condenser and its flow rate is determined from the measurement of the weight of the collected condensate during a given amount of time. The cooling water (5°C), always flows in the annular space counter flow to the air flow. This water temperature was chosen because of the low thermal

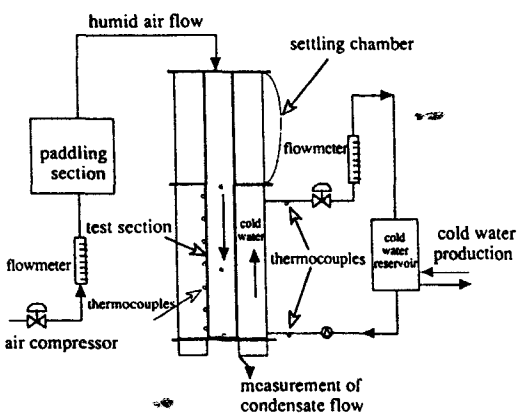

FIG. 3. General experimental setup.

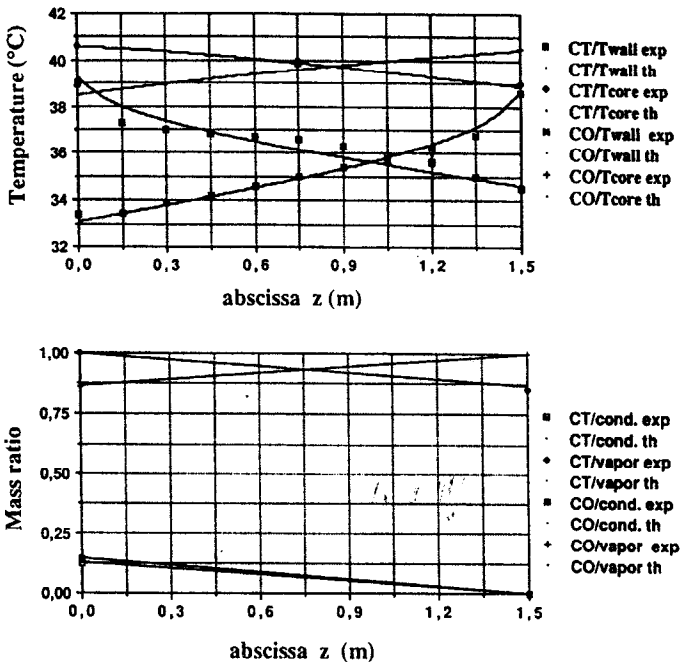

FIG. 4. Comparison of model–experiment results (Re = 33 500, T_c = 40.4°C, T_p = 7°C).

conductivity of "PVC" making up the condenser. The water flow rate is such that the wall temperature of the condenser can be considered uniform.

The temperature measurements are carried out by micro thermocouples K (copper/constantan). These thermocouples are manufactured by a discharge of a capacity between two wires of diameter 0.5 mm. The air temperature is measured by three thermocouples, at the air inlet, in the middle and at the exit of the tube. The local heat flux passing through the wall is measured by three thermocouples which are fixed on the external wall (i.e. the cooling side). Eleven thermocouples are fixed on the internal hot wall. In order to prevent from hydrodynamic interaction between probes, the thermocouples were located at different azimuthal position along the flow. Thermocouple leads of 10 cm length were fixed on the surface of the tube in order to minimize the thermal conduction losses in the wire through the wall.

5. RESULTS

This part presents the results obtained from the experimental setup described in the previous section as well as the comparisons with the numerical results. Complementary experimental results are obtained without a settling chamber. In this case, the experimental conditions are similar to those found in industry.

5.1. *Comparison between theoretical and experimental results*

The results are presented in Fig. 4, where the two flow directions are gathered (the z axis remaining the same for the two flow directions). We observe that the calculated temperature of humid air corresponds to the measured value. We can use the calculated temperature to estimate the local heat flux. The results concerning the mass fraction as well as the temperature distribution of the cooled wall correspond to the numerical values. However, we observe that the experimental values corresponding to the inlet of the tube are lower than the calculated ones. This difference may be due to the large longitudinal temperature gradient present in this area of the tube. The tri-dimensional phenomena which could appear are not taken into account. The mass fractions are the ratio of steam or condensate flow and steam flow at the tube inlet. The temperature at the interface is determined by imposing the equality between the heat flow of the mixture at the interface and the one going through the wall.

5.2. *Influence of the gas flow direction*

The results are presented in Figs. 5–8 which show, respectively, the axial distribution in the middle of the flow, of the heat transfer through the wall and of the mass fractions.

From Figs. 5b and 7b, we can deduce the influence of the inlet temperature on the condensate mass flow rate. As the mass ratio at outlet of the tube is equal at these two temperatures, the condensate mass flow rate is more important at higher temperatures.

The axial evolution of the temperature in the middle of the flow is pratically identical for the two flow directions. In fact, the temperature gradient is tied to the convective heat transfer of the flow and to the sensitive heat flux of the migrant steam through the

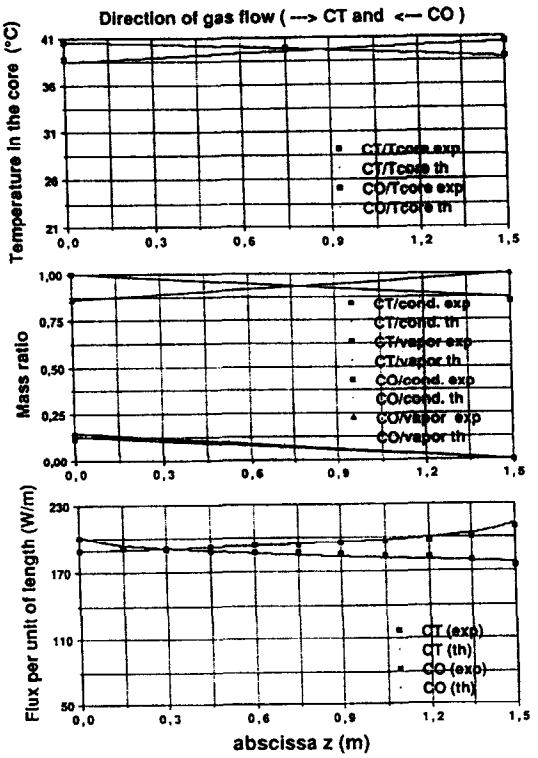

FIG. 5. Comparison of two flow directions ($Re = 33\ 500$, $T_e = 40.4°C$, $T_p = 7°C$).

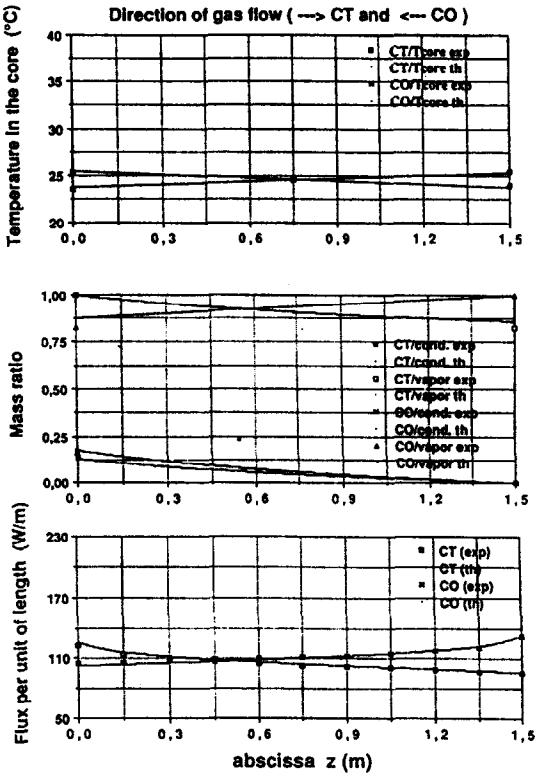

FIG. 7. Comparison of two flow directions ($Re = 34\ 520$, $T_e = 25.3°C$, $T_p = 7.2°C$).

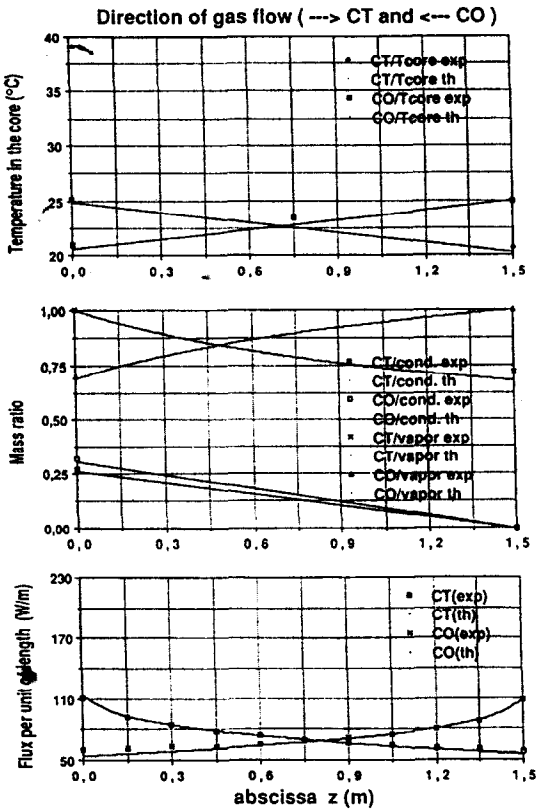

FIG. 6. Comparison of two flow directions ($Re = 11\ 250$, $T_e = 24.9°C$, $T_p = 5°C$).

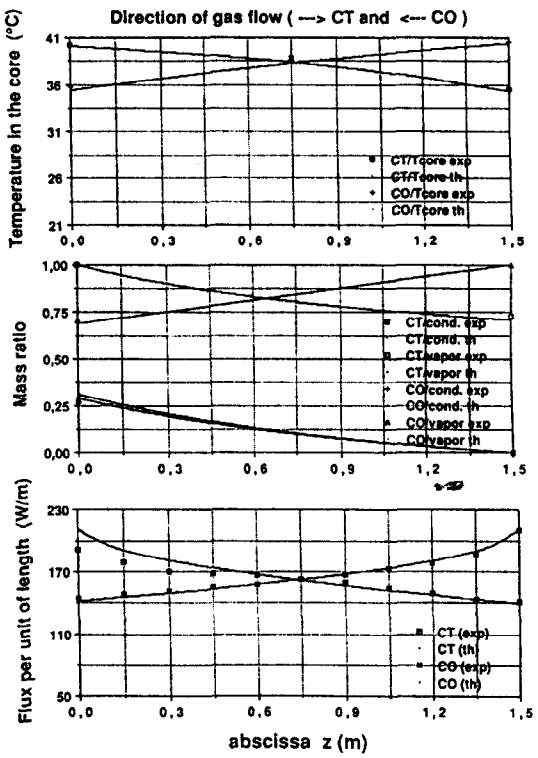

FIG. 8. Comparison of two flow directions ($Re = 11\ 990$, $T_e = 40.1°C$, $T_p = 6°C$).

flow to the interfaces. The small condensation rate (mv_i) has the effect that the convective heat transfer of the flow is predominant and the same for the two flow directions. The sensitive heat transfered in the exchanger is not influenced by the flow direction.

The latent heat flux exchanged in the condenser is directly proportional to the condensate mass fraction. We note that the condensate mass fraction at the tube outlet increases if the flow inlet temperature is raised for the same experimental conditions (Figs. 5b and 7b). The reason being that the condensate flow is directly linked to the temperature difference between the wall and the flow.

In fact, when the steam flow increases, the condensate flow is also increasing, but to a smaller extent. This implies a decrease of the condensate mass fraction (Figs. 5b and 8b). The air is saturated at the tube inlet. The measurement process of the condensate flow was validated by different systems; the measure of the dew-point at the exit seems to be more accurate than the humid temperature measurement. The difference between experimental values and calculated values remains smaller than 10% owing to the great humidity (= 90%) which always remains at the outlet. The measuring device is less accurate in this measurement range. However, only the condensate flow interferes in the calculations.

The axial heat flux through the wall is shown in the lower graphics (Figs. 5–8). We note good agreement between the measured and the calculated values. However, at the tube inlet, the experimental values are lower than the calculated values, the difference remaining less than 7%. These measurements are directly linked to the wall temperature measure, and a conjecture concerning this difference was given in a previous paragraph. The exchanged heat flux through the wall is higher for a parallel flow except for Re = 11 250 and with an inlet temperature of the humid air $T_e = 24.9°C$ (Fig. 6) where the axial evolutions are similar for the two flow directions.

In Table 1 the global internal exchange coefficients for several inlet conditions are listed. Those in the parallel flow direction are higher than those in the counter flow direction. The reason is that the exchanged latent heat transfer is higher. These values are to be compared with the calculated values (cf. Table 2).

5.3. *Experimental tests without settling chamber—comparison between the two flow directions*

The experimental tests are the same as detailed previously. The saturated humid air goes directly into the test section. The model is not representative of the experimental tests without a settling chamber because the model was made for turbulent flow. However, a qualitative comparison is shown in the upper part of Fig. 9. The measured heat transfer flux through the wall is higher than the calculated value for a parallel flow and lower in counter flow. In fact, the difference between the two flow directions increases. In the two other parts of Fig. 9, the difference between the measurements of parallel flow and counter flow becomes significant. The turbulence is probably the reason of this increase. In parallel flow, the turbulence facilitates the condensate flow and decreases the boundary-layer thickness, thus permitting a greater heat transfer. In counter flow, the boundary-layers thicknesses are also smaller, but the condensate flow is showed by the air flow increasing its thickness. The heat transfer flux through the wall is then lower.

During these tests, some waves appear on the condensate surface, particularly in counter flow when the condensate thickness is greater. In counter flow, for Re = 33 500 and $T_e = 40.4°C$, too little condensate was recovered at the tube exit. We can explain this particularity by the equality in absolute value of the condensate mass and the shear stress at the interface.

In Table 2 the global internal exchanger coefficients are given. We note an increase of parallel flow values and a great decrease in counter flow compared to the tests with a settling chamber. During a test without a settling chamber, the shear stress at the gas–condensate interface is more important because of the turbulence. So, in cocurrent flow, the thickness of the condensate is lower than with a settling chamber, and the heat transfer is higher. In counter flow the phenomena are opposite. The global internal transfer coefficient increases with the temperature for a given velocity (see Tables 1 and 2). But, without a settling chamber test, at 17 m s^{-1} in a counter current, this coefficient decreases. The reason is that the thickness of the condensate increases with the inlet temperature, and becomes as important, and this thermal resistance is no longer negligible. So the internal coefficient decreases.

Table 1. Comparison of the global internal exchange coefficients for different inlet conditions with settling chamber (*co*: parallel flow direction, *ct*: counter flow direction)

u (m s^{-1})	6		11		17	
Re	11 200		24 200		34 500	
($T_c = 25°C$)						
T_e (°C)	*co*	*ct*	*co*	*ct*	*co*	*ct*
25	105	97	205	188	270	214
35	155	142	284	204	401	250
40	213	176	355	249	498	342

Table 2. Comparison of the global internal exchange coefficients for different inlet conditions without settling chamber (*co*: parallel flow direction, *ct*: counter flow direction)

u (m s^{-1})	6		11		17	
Re	11 200		24 200		34 500	
($T_c = 25$°C)						
T_c (°C)	*co*	*ct*	*co*	*ct*	*co*	*ct*
25	127	76	234	105	312	94
35	176	104	394	128	508	70
40	225	111	526	183	609	50

Summarizing, the experimental results confirm the model conclusions. The gas/condensate parallel flow allows for a better recovery of heat energy. The absence of the settling chamber allows the increase of heat transfer in parallel flow and its decrease in counter flow.

6. CONCLUSION

The work presented in this paper takes place in the general context of the heat and mass transfer modeling study on the effect of humid air flow rate on the filmwise condensation inside a vertical cooled pipe, in turbulent forced convection.

The optimum energy recovery in the condenser is conditioned by:

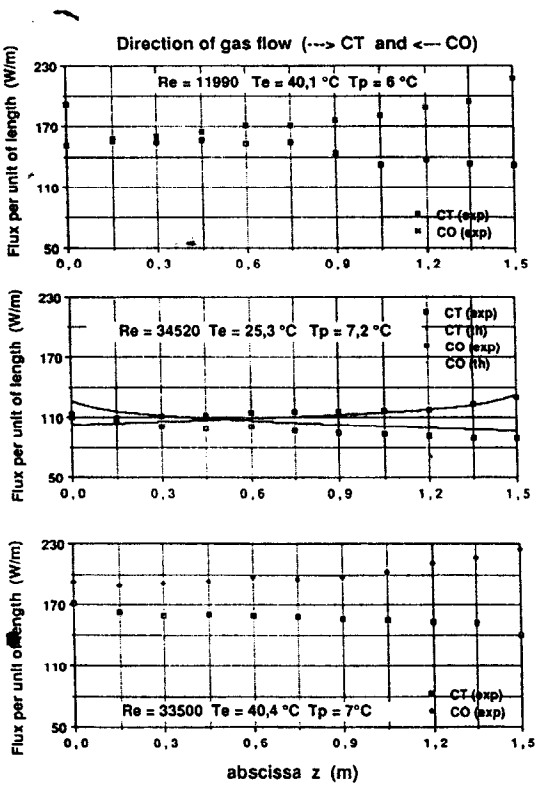

FIG. 9. Experimental tests without surge chamber. Comparison of two flow directions.

- the accumulation of non-condensing gas near the liquid film; and
- the condensate film thickness which is a function of its mass and of the shear stress at the gas–condensate interface.

The theoretical results show a difference between the two flow directions which is increased when the speed or the temperature of the flow increases. The parallel flow direction allows for a better energy recovery.

All the experimental results correspond to the numerical simulation. Moreover, the entry effects on the exchanger coefficients are significant, which justifies the characterization of the axial distribution of the diffusion coefficient.

Another test series was carried out without a settling chamber in order to find the best industrial condition. The difference increased. In parallel flow, the results without a settling chamber were better than those with a settling chamber. However, no comparison is possible with the theoretical model.

These results, which show an increase of the mass transfer in the two flow directions when the humid air flow increases, are similar to those of Hikita *et al.* [10]. This work completes the results already published because here we change the inlet temperature of the humid air. Moreover, the condensate flow is controlled by certain physical phenomena (condensation and shear stress at the gas–liquid interface) and not by the operator.

Finally, we have remarked the importance of the entry conditions (temperature and flow) on the heat and mass exchanges. This point is of great importance for industrial applications.

REFERENCES

1. R. G. Owen and W. C. Lee, A review of some recent developments in condensation theory, *IChemE Symp. Ser.* **75** (1984).
2. A. P. Colburn and O. A. Hougen, Design of cooler condenser for mixtures of vapors with noncondensing gases, *Ind. Engng Chem.* **26**, 1178–1172 (1934).
3. A. P. Colburn and T. B. Drew, The condensation of mixed vapors, *Trans. A.I.Ch.E.* **33**, 197–215 (1937).
4. F. Legeay-Desquelles, Etude théorique et expérimentale du transfert de chaleur et de masse dans une couche limite incompressible avec condensation sur une plaque

plane, Thèse, Université Pierre et Marie Curie, Paris 6 (1984).
5. Y. R. Mayhew and J. K. Aggariwal, Laminar film condensation with vapour drag on a surface, *Int. J. Heat Mass Transfer* **16,** 1944–1949 (1973).
6. R. B. Bird, W. E. Stewart and E. N. Lightfoot, *Transport Phenomena*. John Wiley, New York (1960).
7. J. Merigoux, Transmission de la chaleur à l'évaporateur, *Intiation aux Transfert Thermiques—Technique et Documentation* (Edited by J. F. Sacadura), Chapter 3 (1978).
8. A. C. Bannwart, Etude théorique et expérimentale de la condensation d'une vapeur en présence d'incondensables. Proposition d'un modèle de film gazeux en convection forcée turbulente, Thèse, Institut National Polytechnique de Grenoble (1984).
9. C. Pele, Influence du sens d'écoulement de l'air humide sur la condensation en film dans un condenseur monotubulaire vertical, Thése, l'ust Lille (1990).
10. H. Hikita, K. Ishimi and H. Ikeki, Mass transfer into turbulent gas streams in wetted-wall columns with cocurrent and countercurrent gas liquid flow, *J. Chem. Engng Japan* **11** (1978).